第 31 卷第 5 期 无 机 化 学 学 报 Vol.31 No.5
2015 年 5 月 CHINESE JOURNAL OF INORGANIC CHEMISTRY 989-1002

载体材料对单 Pd 三效催化剂性能及催化活性的影响

崔亚娟[1] 方瑞梅[2] 尚鸿燕[2] 史忠华[3,4,5] 龚茂初[3,4,5] 陈耀强*[,1,2,3,4,5]
([1]四川大学建筑与环境学院,成都 610065)
([2]四川大学化学工程学院,成都 610065)
([3]四川大学绿色化学与技术教育部重点实验室,成都 610064)
([4]四川省机动车尾气净化工程技术研究中心,成都 610064)
([5]四川省环境保护环境催化材料工程技术中心,成都 610064)

摘要: 采用共沉淀法制备了耐高温高比表面的 La_2O_3-Al_2O_3(LA)以及铈含量分别为 15%、33%和 47%的储氧材料 CeO_2-ZrO_2-La_2O_3-Al_2O_3(CZLA)、CeO_2-ZrO_2-La_2O_3+La_2O_3-Al_2O_3(CZL+LA)和 CeO_2-ZrO_2-La_2O_3(CZL)4 类载体材料,并用浸渍法制备了整体式 Pd/LA、Pd/CZLA、Pd/CZL+LA 和 Pd/CZL 汽油车尾气净化三效催化剂,考察了载体材料对单 Pd 三效催化剂的影响。采用低温 N_2 吸附–脱附、H_2-程序升温还原(H_2-TPR)以及 X 射线光电子能谱(XPS)对载体材料及催化剂进行了表征,并考察了催化剂的空燃比性能和三效催化性能。结果表明,CZLA 有效地结合了铈基和铝基载体材料的优点,表现出了优异的织构性能、热稳定性及还原性能。老化前后,其负载的单 Pd 三效催化剂在低温还原率、表面元素含量及 Pd 的电子结合能等性能方面表现出了最小的差异。催化剂活性测试结果表明,Pd/CZLA 的三效窗口明显较宽,且拥有最低的起燃温度,尤其经 1 000 ℃老化处理后,其催化活性最高,C_3H_8、NO_x 和 CO 的起燃温度分别为 370、257 和 223 ℃。可见,相较于其他 3 种载体材料,CZLA 更适合于负载单 Pd 三效催化剂,从而满足更高标准的三效催化剂的性能要求。

关键词: 钯; 催化剂; 多相催化; 载体材料; 织构性能; 热稳定性; 单 Pd 三效催化剂; 催化性能。
中图分类号: O643.36; O614.82+3; O614.33+2; O614.41+2 **文献标识码**: A **文章编号**: 1001-4861(2015)05-0989-14
DOI: 10.11862/CJIC.2015.120

Effect of Support Materials on Property and Catalytic Performance of Pd-Only Three-Way Catalyst

CUI Ya-Juan[1] FANG Rui-Mei[2] SHANG Hong-Yan[2] SHI Zhong-Hua[3,4,5] GONG Mao-Chu[3,4,5]
CHEN Yao-Qiang*[,1,2,3,4,5]
([1]*College of Architecture and Environment, Sichuan University, Sichuan, Chengdu* 610065, *China*)
([2]*College of Chemical Engineering, Sichuan University, Sichuan, Chengdu* 610065, *China*)
([3]*Key Laboratory of Green Chemistry & Technology, Ministry of Education, College of Chemistry, Sichuan University, Sichuan, Chengdu* 610064, *China*)
([4]*Center of Engineering of Vehicular Exhaust Gases Abatement, Sichuan Province, Sichuan, Chengdu* 610064, *China*)
([5]*Center of Engineering of Environmental Catalytic Material, Sichuan Province, Sichuan, Chengdu* 610064, *China*)

Abstract: Four kinds of support materials, i.e. a thermally stable material La_2O_3-Al_2O_3(LA), three oxygen storage materials CeO_2-ZrO_2-La_2O_3-Al_2O_3(CZLA), CeO_2-ZrO_2-La_2O_3+La_2O_3-Al_2O_3(CZL+LA) and CeO_2-ZrO_2-La_2O_3(CZL) with ceria content of 15%, 33% and 47%, respectively, were prepared by co-precipitation. The corresponding Pd-only catalysts Pd/LA, Pd/CZLA, Pd/CZL+LA and Pd/CZL were obtained by wet-impregnation and further fabricated as three-way catalysts in a monolith form. The support materials were characterized by low temperature nitrogen

收稿日期:2014-11-08。收修改稿日期:2015-02-13。
国家自然科学基金(No.21173153),四川省科技厅科技支撑项目(2011GZ0035)资助。
*通讯联系人。E-mail:nic7501@scu.edu.cn

adsorption-desorption and H_2-temperature programmed reduction (H_2-TPR). The catalysts were characterized by H_2-TPR and XPS, and were evaluated with a simulated automobile exhaust in terms of the relationships of three way performance with the air/fuel operation window and with temperatures. The results indicate that the support material CZLA integrates the advantages of ceria-based and alumina-based materials effectively thus having superior textural property, thermal stability and reduction property. Additionally, Pd/CZLA catalyst shows little difference in low temperature reducibility, surface elemental distribution and elemental oxidation states before and after aging treatment. As a result, Pd/CZLA exhibits the widest air/fuel operation window and the lowest light-off temperature among the four catalysts, especially after aging treatment, the light-off temperature of C_3H_8, NO_x and CO is 370 ℃, 257 ℃, 223 ℃, respectively. Then material CZLA is the most suitable support for Pd-only three-way catalyst compared with the other three supports.

Key words: palladium; catalysts; Heterogeneous catalysis; support materials; textural properties; thermal stability; Pd-only three-way catalysts; catalytic performance.

0 Introduction

Environmental protection has attracted worldwide attention in the past decades. The pollutant emissions mainly composed of hydrocarbons (HC), CO and NO_x from gasoline engine powered vehicles is a major cause of air pollution[1]. Further work should be done to purify the aforementioned contaminations simultaneously and to meet emission limits in the future. Three-way catalysts (TWCs) commercialized in the USA and Japan since 1977 have been the most satisfactory and efficient techniques to convert the emissions of HC, CO and NO_x to harmless products CO_2, N_2 and H_2O [1-2]. Clearly, there has been a continuous evolution of TWCs technology in the last 30 years, leading to more and more efficient TWCs[3-4]. The combined requirements of compactness, high volumetric ow rates and low back pressure lead to the universal adoption of monolithic catalysts for automotive catalysts [3]. Conventional monolithic three-way catalysts are mainly made up by catalyst matrix, support materials, active components including noble metals Pt, Pd, Rh, etc and/or catalyst additives[5-6]. Pd-only/Pd-rich TWCs have received considerable attention because of its noticeable advantages, such as the comparatively low cost, rich abundance, excellent low-temperature oxidation activity for CO and hydrocarbons, etc[7]. Additionally, the stability and NO selective reduction of Pd-only can be enhanced by improving the support material. By studying different mixing strategies of $Ce_{0.5}Zr_{0.5}O_2$ (CZ) and Al_2O_3, Lan and coworkers[8] have concluded that the modied co-precipitation method can improves the textural, structural and reduction properties of the support $Ce_{0.5}Zr_{0.5}O_2$-Al_2O_3, leading to enhance the thermal stability of Pd-only catalyst. According to the work reported by Talo et al.[9], the promoters of Zr, Si, La, and Ba can influence the anti-aging performance of Pd-only catalysts. Cai et al.[10] have reported that the doping of less than 10% BaO in the Ce-Zr system can form the stable CZB solid solution, and this support helps the Pd-only catalyst hold high thermal stability and NO selective reduction. Also, Iwamoto et al.[11] have reported that catalysts containing Mg, Ba and Ca can obviously improve the reduction conversion of NO to N_2.

For final TWCs, the support material greatly affects the performance of the catalyst, because it can provide surroundings where the active compound remains in the form of small particles and increases thermal stability of the active compound[12]. At present, the TWCs support materials mainly include the following types: (i) γ-Al_2O_3 stabilized by alkaline earth metals and rare earth elements[13-14]; (ii) CeO_2-based oxygen storage material (OSM) [15-16]. However, the significant loss of the OSM property due to aging at

high temperatures is still a major drawback of OSM; (iii) ACZ-type material (Al_2O_3-CeO_2-ZrO_2) which was practically applied in TWCs as OSM in 2001[17]. The material exhibits high thermal stability and superior redox properties incorporating the advantages of alumina-based and ceria-based materials.

As described above, various support materials possess different properties. Consequently, active components should be loaded on corresponding supports, which depends on intended application, emissions and technical requirements. In the present work, four kinds of support materials, LA, CZLA, CZL+LA and CZL prepared by co-precipitation were used as the support material for Pd-only catalysts. Then, the performance of the supports and catalysts was investigated and discussed. At last, the optimal support material for Pd-only catalyst was obtained.

1 Experimental

1.1 Synthesis of support materials

The support materials of La_2O_3-Al_2O_3(weight ratio 3:97), CeO_2-ZrO_2-La_2O_3-Al_2O_3 (weight ratio 15:15:5:65) and CeO_2-ZrO_2-La_2O_3 (weight ratio 47 :47 :6) were prepared by co-precipitation from the corresponding chemicals (Chengdu Kelong Chemical): $Ce(NO_3)_3 \cdot 6H_2O$, $ZrO(CO_3)$ (dissolved with HNO_3 with mass fraction of 65%~68%), $La(NO_3)_3 \cdot 6H_2O$, $Al(NO_3)_3 \cdot 9H_2O$ at the appropriate ratios. The precursors were mixed in an aqueous solution, separately. Then, the aqueous solutions were precipitated with ammonia solution (25wt%) under vigorous stirring and the pH value was kept at around 9.0 during the process. Afterwards the precipitates were filtered, washed with distilled water, dried at 120 ℃ overnight, and calcined at 600 ℃ in air for 3 h to get the final support materials. CeO_2-ZrO_2-La_2O_3 (weight ratio 47:47:6)+La_2O_3-Al_2O_3 (weight ratio 3 :97) was synthesized by simultaneous coprecipitation. Ce-Zr-La (70wt%) mixed solution and La-Al (30wt%) mixed solution were obtained, separately. Then the two solutions were simultaneously precipitated with ammonia solution (25wt%), at the same time, the precursors were mixed thoroughly through vigorous stirring. The obtained precipitate was treated in the same way as described above. The final support materials La_2O_3-Al_2O_3, CeO_2-ZrO_2-La_2O_3-Al_2O_3, CeO_2-ZrO_2-La_2O_3 +La_2O_3-Al_2O_3 and CeO_2-ZrO_2-La_2O_3 were marked as LA, CZLA, CZL +LA and CZL, respectively. The materials calcined at 600 ℃ for 3 h are designated as the fresh supports in this work, while the aged supports are those by thermal treating the fresh supports at 1 000 ℃ for 5 h.

1.2 Preparation of TWCs

The corresponding Pd-only TWCs were prepared by impregnating the fresh support material powders with aqueous solution of $Pd(NO_3)_2$ (the mass fraction of Pd is 17.0%), and the theoretical loading of Pd was 1.0wt% for all catalysts. Then the impregnated powders were calcined at 550 ℃ for 3 h. Thereafter the powders were mixed with distilled water to obtain slurries which were spread to a honeycomb cordierite (Corning, USA, 400 cells·in.$^{-2}$, 2.5 cm^3) and excessive slurry was blown away with compressed air. The obtained catalysts were labeled as Pd/LA, Pd/CZLA, Pd/CZL +LA and Pd/CZL. The fresh catalysts were obtained by calcining the prepared catalysts at 550 ℃ for 3 h, and the aged catalysts were obtained by thermal treating the fresh catalysts at 1 000 ℃ for 5 h.

1.3 Activity tests of TWCs

The catalytic performance of TWCs was evaluated in a multiple fixed-bed continuous flow microreactor by passing a feed stream similar to that of an exhaust from a gasoline engine. The feed stream was regulated with mass-flow controllers before entering the blender. The simulated exhaust gases were composed of CO(0.42%), C_3H_8(0.05%), NO (0.06%), CO_2(12%), H_2O(10%), O_2(adjustable) and balanced with N_2 at a gas hourly space velocity of 34 000 h^{-1}. The concentrations of the effluent C_3H_8, NO_x and CO were analyzed by a five-component analyzer (FGA-4100, Foshan). Before each measurement the catalyst was pretreated under the reactive gas mixture at 550 ℃ for 1 h.

1.4 Characterization techniques

The textural properties were analyzed by N_2 adsorption-desorption at 77 K using a Quantachrome

automated surface area & pore size analyzer (Autosorb SI). The specific surface area and pore size distribution were calculated by BET and BJH models. All supports were degassed at 300 ℃ for 3 h under vacuum prior to the measurement.

Hydrogen-temperature programmed reduction (H_2-TPR) for all supports and catalysts were carried out on a self-assembled device equipped with a gas chromatograph. Before the H_2-TPR experiment, 100 mg sample in granules of 841~420 μm (20~40 mesh) was pretreated with a flow of N_2 (25 mL·min^{-1}) at 400 ℃ for 1 h, after cooling down to room temperature, the sample was heated under a flowing N_2-H_2 gas mixture of 5vol% H_2 (20 mL·min^{-1}) at a heating rate of 8 ℃·min^{-1}. The consumption of H_2 was monitored by a thermal conductivity detector (TCD).

The X-ray photoelectron spectroscopy (XPS) experiments were carried out on a spectrometer (XSAM-800, KRATOS Co) with Mg *Kα* radiation ($h\nu$= 1 253.6 eV) under ultra-high vacuum condition. The XPS data related to Ce3*d*, Zr3*d*, La3*d*, Al2*p*, O1*s* and Pd3*d* core levels were recorded for all catalysts. The surface charging effect was corrected by fixing the C1*s* peak at a binding energy of 284.6 eV.

The metal dispersion of palladium was determined by CO chemisorption. Approximately 300 mg sample was placed in a U-shaped quartz tube. Prior to chemisorption, the catalyst was reduced in a flow of H_2 (20 cm^3·min^{-1}) at 400 ℃ for 1 h, then purged with pure Ar (30 mL·min^{-1}). After cooling down to room temperature, carbon monoxide was pulsed and detected by TCD.

2 Results and discussion

2.1 Three-way catalytic activity

The results of air/fuel ($S=(2C_{O_2}+C_{NO})/(10_{C_3H_8}+C_{CO})$) over fresh and aged catalysts are shown in Fig.1, and S>1 is lean (less fuel and more air) while S<1 is rich (more fuel and less air). Observing Fig.1 (a), for fresh catalysts Pd/CZLA and Pd/CZL+LA, the conversion of C_3H_8 achieves 100%, but there is slight decrease under rich condition for Pd/CZL+LA. The conversion of C_3H_8 for Pd/CZL increases with the increase of S value until achieving 100%, while for Pd/LA, it presents a trend of increasing first and then decreasing. This behavior indicates that Pd/CZLA and Pd/CZL+LA facilitate the reaction of steam reforming of C_3H_8, which makes the conversion of C_3H_8 achieve

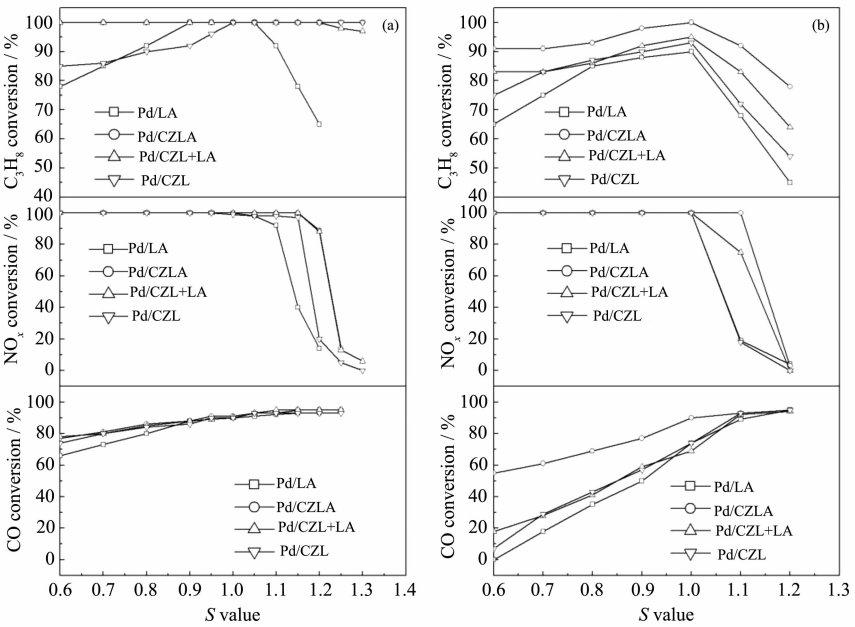

Fig.1 Variations of the conversion of C_3H_8, CO and NO_x in the simulated automobile exhaust with the air to fuel ratios (S value) over fresh (a) and aged (b) catalysts

100% under lean condition. The NO_x conversion is 100% under $S \leqslant 1$ condition but decreases obviously with increasing S value under $S>1$ condition for all the fresh catalysts. The NO_x operation windows for Pd/CZLA and Pd/CZL+LA are the widest while it is the narrowest for Pd/LA. With regard to CO conversion, it increases with increase of S value until the conversion is higher than 90%, and all fresh catalysts show similar catalytic activity for CO oxidation except for Pd/LA which exhibits slightly worse conversion under lean oxygen condition.

In the case of aged catalysts, the widths of the C_3H_8, NO_x and CO operation windows all become narrower than those of fresh catalysts due to sintering, but the law of catalytic activity on different catalysts is similar to that of fresh catalysts. As shown in Fig.1 (b), for C_3H_8 oxidation the catalytic activity still follows the sequence of Pd/CZLA >Pd/CZL +LA >Pd/CZL>Pd/LA in the whole S value range. With regard to NO_x conversion, the width of operation window for Pd/CZLA is wider than that of Pd/CAL +LA. The widths of NO_x operation window on Pd/LA and Pd/CZL are similar but the narrowest among all these catalysts. As for the CO oxidation, the catalytic activity for Pd/CZLA is obviously more superior to that of the other three catalysts. The observation presented above shows that Pd/CZLA exhibits wider air/fuel operation window than the others especially for aged catalysts.

The catalytic performance of fresh and aged catalysts is investigated at S value=1 and the results are shown in Fig.2. Obviously, the conversion temperatures of the three pollutants increase in the order of C_3H_8 >NO_x >CO. For fresh catalysts, Pd/LA exhibits the worst catalytic activity, implying the inferiority of the LA as the support for palladium. According to previous study[18-19], the addition of suitable cerium to the catalytic support can enhance the conversion of C_3H_8 and NO_x, but excess cerium can inhibit the adsorption of C_3H_8 pollutant which will affect the oxidation activity of C_3H_8. In our work, for the three ceria-containing catalysts, the catalytic activities of C_3H_8 and NO_x are in the sequence of Pd/CZLA >Pd/CZL +LA >Pd/CZL, indicating that the material CZLA (cerium content of 15%) is the best support of palladium for C_3H_8 and NO_x conversion. As for CO conversion, Pd/CZL +LA exhibits slightly higher catalytic activity than Pd/CZLA. The third is

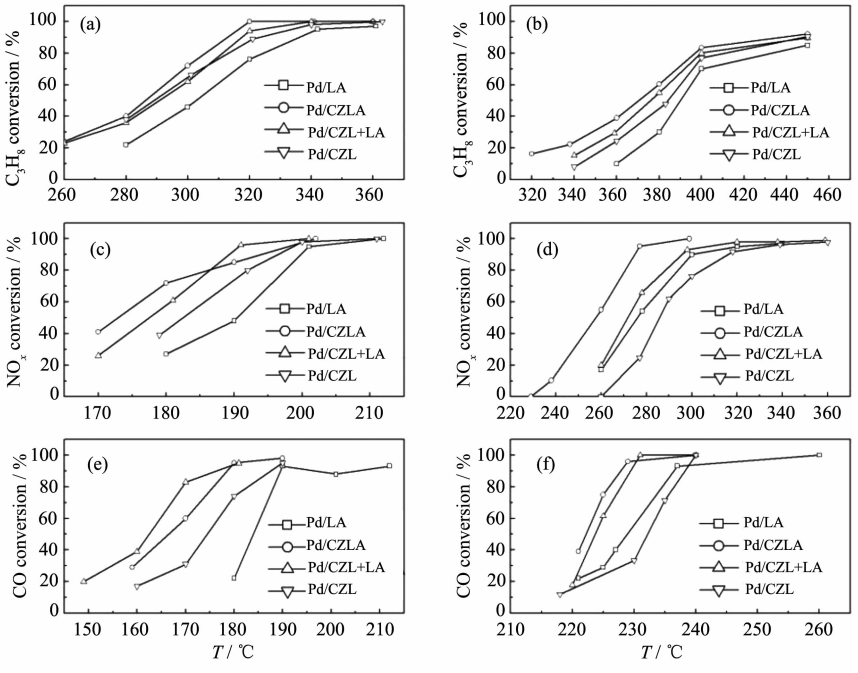

Fig.2　Conversion curves of C_3H_8, NO_x and CO as a function of temperature over the fresh (a, c, e) and aged (b, d, f) catalysts

Pd/CZL and the worst is Pd-LA. For aged catalysts, a large drop of activity is observed compared with fresh ones, attributing to the deteriorated structure and the sintering of active component[1]. Observing Fig.2(b), the catalytic behaviors of the aged catalysts are slightly different from their corresponding fresh comparatives. The catalytic activities of C_3H_8 are in the sequence of Pd/CZLA>Pd/CZL+LA>Pd/CZL>Pd/LA, while for the conversion of NO_x and CO, it increases in the order of Pd/CZLA>Pd/CZL+LA>Pd/LA>Pd/CZL. It is worth noting that Pd/CZLA exhibits the best catalytic activity for all the three pollutants elimination.

With regard to the light-off temperatures (T_{50}, the temperature required to attain 50% conversion) for C_3H_8, NO_x and CO over the four catalysts in Fig.3, the change trend is similar to that of the catalytic activity. For the fresh catalyst Pd/LA in Fig.3(a), the light-off temperatures for C_3H_8, NO_x and CO are 303, 190 and 184 ℃, respectively, which are the highest among the four fresh catalysts. As for the ceria-containing catalysts, the light-off temperatures of C_3H_8 and NO_x over Pd/CZLA are 286 and 173 ℃, respectively, which are the lowest. While for CO, they follow the sequence of Pd/CZL (174 ℃)>Pd/CZLA (166 ℃)>Pd/CZL+LA(163 ℃). In the case of aged catalysts, the light-off temperatures of the three pollutants are higher than that of fresh catalysts. But for aged Pd/CZLA, the light-off temperatures of C_3H_8, NO_x and CO are 370, 257, 223 ℃, respectively, which still are the lowest than the three others.

2.2 Textural properties of support materials

As shown in Table 1, the values of BET surface area (S_{BET}) and cumulative pore volume of the fresh supports increase with the increasing of aluminum content. And the supports LA and CZLA exhibit the biggest value of average pore radius about 5.8 nm. After aging treatment, all supports experience a

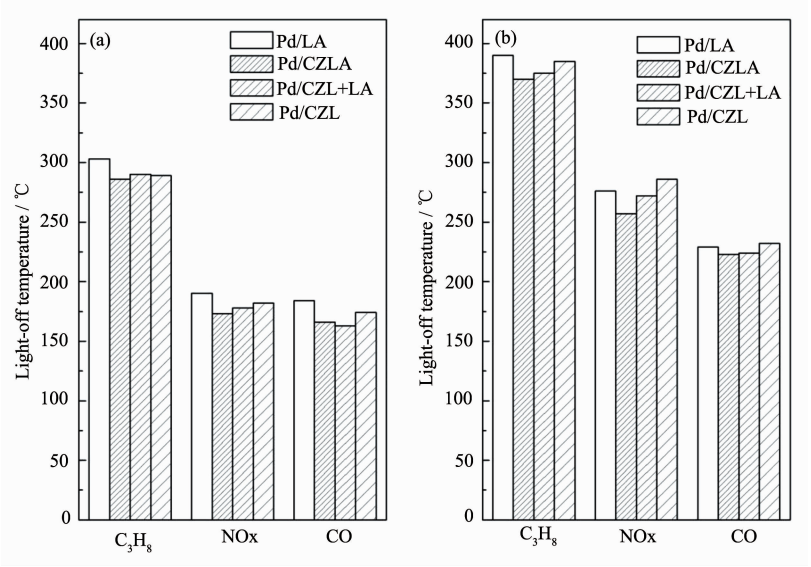

Fig.3 Light-off temperatures for C_3H_8, NO_x and CO over the fresh (a) and aged (b) catalysts

Table 1 Textural properties of fresh and aged supports

Sample	Fresh			Aged		
	S_{BET} / ($m^2 \cdot g^{-1}$)	Pore volume / ($cm^3 \cdot g^{-1}$)	Average pore radius / nm	S_{BET} / ($m^2 \cdot g^{-1}$)	Pore volume / ($cm^3 \cdot g^{-1}$)	Average pore radius / nm
LA	292	0.73	5.7	138	0.57	8.8
CZLA	254	0.60	5.8	108	0.43	8.0
CZL+LA	168	0.44	5.2	57	0.22	8.6
CZL	94	0.23	4.1	26	0.08	8.4

reduction of S_{BET} and total pore volume due to severe sintering when the supports are exposed to high temperature. However, LA and CZLA still maintain high S_{BET} values which are 138 and 108 $m^2 \cdot g^{-1}$ respectively. While CZL remains only 26 $m^2 \cdot g^{-1}$ and the value of pore volume is only 0.08 $cm^3 \cdot g^{-1}$ which is far less than that of LA and CZLA. Additionally, compared with the fresh state, the percentage area loss upon heat treatment at 1 000 ℃ for LA, CZLA, CZL+LA and CZL are 53%, 57%, 66% and 72%, respectively. The loss of S_{BET} is disadvantageous for the dispersion of precious metals. The average pore radii of aged supports increase to some extent compared with those of fresh supports and the values are in the range of 8~9 nm. This can be attributed to the coagulation of nanoparticles leading to particle growth and thus to elimination of small radii pores and formation of bigger ones[20].

Fig.4 displays the representative N_2 adsorption-desorption isotherms of fresh and aged supports. All the isotherms belong to type Ⅳ (IUPAC classication) with a hysteretic loop characteristic of mesoporous solids. For fresh supports, the hysteretic loop of CZL can be ascribed to H2-type, implying the present of typical conterminous mesopores[21]. The other three supports which contain variant amounts of alumina show H1-type hysteretic loop, indicating the formation of large interparticle mesopores both at the external surface and in the inner region of the agglomerate[22]. After calcination at 1 000 ℃ for 5 h, all the relative pressure values for the closing of hysteretic loop shift to higher values compared with those of fresh supports, indicating the formation of bigger pore radius because of sintering at high temperature, which is in accordance with the textural property results. Moreover, the type of hysteretic loop for CZL shifts from H2 to H1 while other three supports maintain previous types, implying that the thermal stability of alumina-containing materials is more superior to that of material free from alumina.

Fig.5 shows the pore size distributions (PSDs) for the fresh and aged supports. For fresh supports, LA, CZLA and CZL +LA show similar pore structure presenting a PSD characterized by a first peak at 2.5 nm and a second peak at 5.5 nm, while for CZL, there are first weak peak at 2.5 nm and second peak at 3.9 nm. Clearly, the width of PSDs increases with the increase of aluminum content. Upon thermal treatment, all pore structures are wrecked to some extent especially for CZL. And all PSDs exhibit a shift of the pore radius to higher values, resulting from elimination of small radii pores and formation of

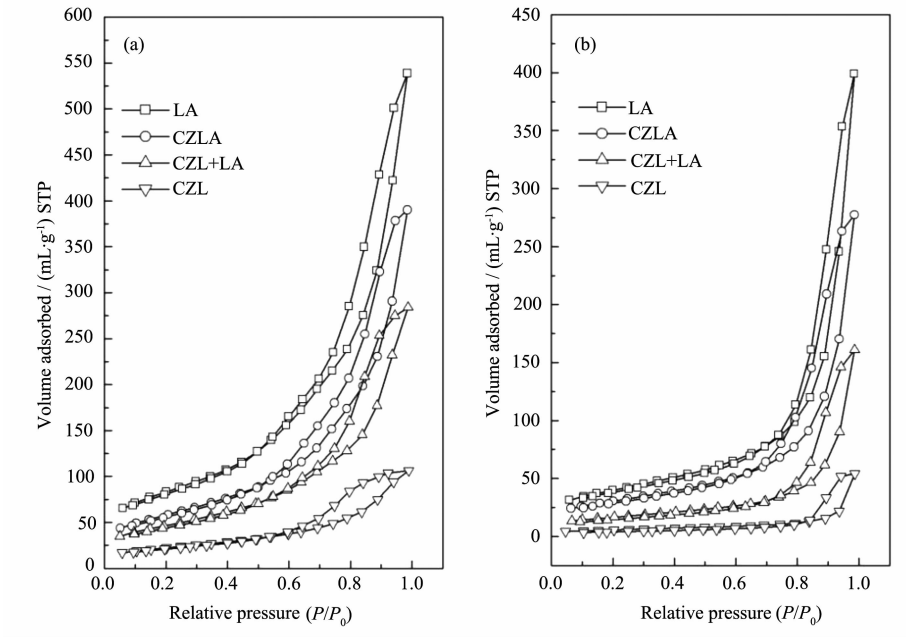

Fig.4　N_2 adsorption-desorption isotherms of (a) fresh and (b) aged supports

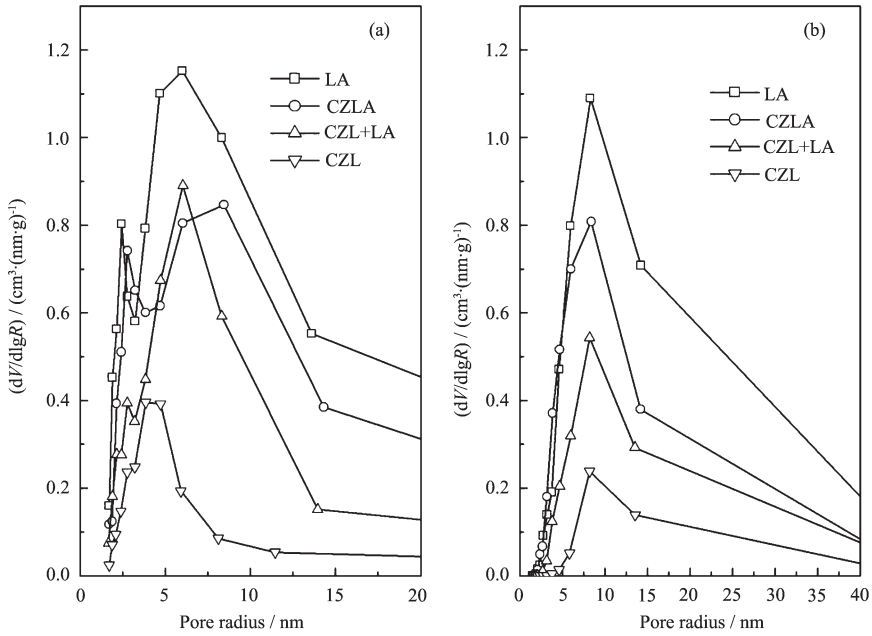

Fig.5 Pore size distributions of (a) fresh and (b) aged supports

bigger ones. Moreover, the PSDs of aged supports become one broad peak, which is mainly in the range of 4~20 nm. Similar to fresh samples, the PSDs of alumina-containing supports are wider than that of support free of alumina.

Accordingly, the excellent catalytic activity for Pd/CZLA partly attributes to the high surface area, high pore volume and wide pore size distribution of CZLA support which is beneficial to the adsorption/desorption of target pollutant [23-24]. Additionally, the superior thermal stability of CZLA is an important factor to maintain the aged catalyst Pd/CZLA with high catalytic activity.

2.3 Reduction features of support materials and TWCs

The reduction features of fresh and aged supports are determined by H_2-TPR measurement and the results are shown in Fig.6. Obviously, there is no reduction peak for LA before and after aging treatment because both the La_2O_3 and Al_2O_3 supports are difficult to reduce under this condition and no reduction species can be detected. The other three supports with various ceria show the similar reduction profiles, and a strong reduction peak with a shoulder on the low temperature side can be observed. Typically, pure ceria gives the dual-peak TPR signal attributed to surface (peak near 500 ℃) and bulk (peak near 800 ℃) reduction[25-26]. However, the reduction of the bulk lattice oxygen in cerium-zirconium solid solution becomes easier because of the distortion of the structure, which makes it occur simultaneously with the reduction of surface oxygen[27]. This indicates that all CZLA, CZL +LA and CZL are form homogeneous CZ solid solutions regardless of ceria content. The shoulder peak may be attributed to the reduction of subsurface Ce^{4+} species, or perhaps some crystalline CeO_2 is highly dispersed on the surface particles, leading to enhanced low- temperature reducibility[28]. As shown in Fig.6(a), the amount of H_2 consumption increases with the increases in cerium content, nevertheless the reduction temperature of the strong reduction peak increases in the order of CZL (593 ℃)>CZL+LA (579 ℃)>CZLA (571 ℃). The sequence of the reduction temperature is the same as that of surface area and pore volume, i.e. the larger surface area and pore volume of CZLA will promote the reduction ability at low temperature[29].

As shown in Fig.6(b), slight change can be

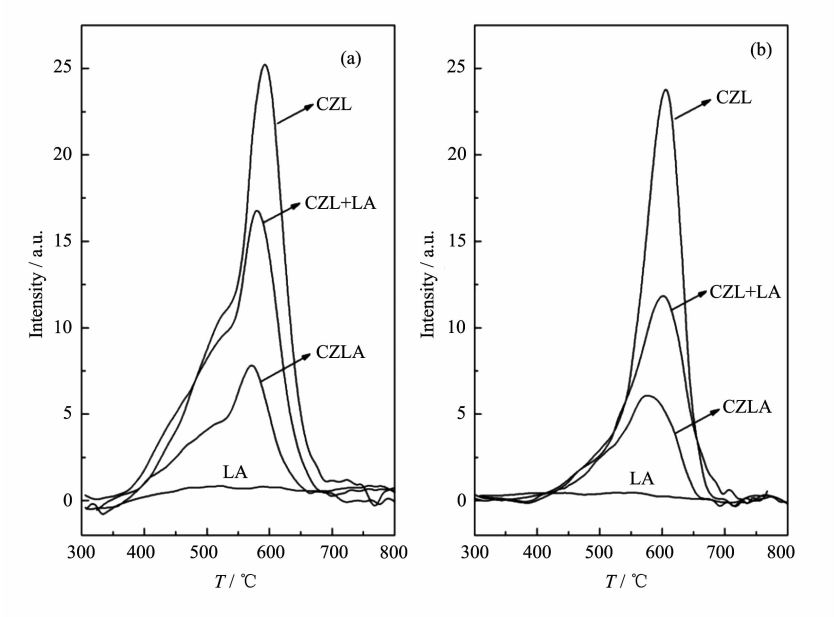

Fig.6　H_2-TPR profiles of the (a) fresh and (b) aged supports

observed after aging treatment. The total peak area of TPR proles decreases because of textural structure destruction. Especially for CZL +LA and CZL, the shoulder peaks almost disappear, while the CZLA still maintains a large shoulder peak. Additionally, the reduction temperatures of the strong reduction peak for CZL, CZL+LA and CZLA are 605, 603 and 575 ℃ respectively. The peaks of CZL and CZL +LA shift towards higher temperature, while the peak of CZLA is nearly unaltered, implying the excellent reduction property of CZLA benefited from the prominent thermos-stability as confirmed by textural property results.

The TPR proles of fresh and aged catalysts are shown in Fig.7. In contrast to blank supports, the reduction peak in the temperature range of 400~700 ℃ disappears (this part is not included in the gure) and a new feature below 200 ℃ appears. According to previous studies[30-31], the reduction peaks below 200 ℃ are assigned to the reduction of PdO species. And the amount of H_2 consumption increases in the order of Pd/CZL >Pd/CZL +LA >Pd/CZLA >Pd/LA, which is similar to that of fresh supports. Furthermore, for the catalysts Pd/CZLA, Pd/CZL +LA and Pd/CZL, the amount of H_2 consumption is more than the sum of the theoretical value attributed to reduction of PdO alone, due to the greater contribution of oxygen from the supports[25]. The shift to lower temperature for the reduction of CeO_2-ZrO_2 is attributed to the presence of Pd which promotes the back-spillover process of oxygen from the support to PdO surface[32-33]. After aging treatment, there are remarkable changes in the reduction features for all catalysts. Two reduction peaks (α and β) can be seen below 200 ℃ for Pd/CZLA, Pd/CZL+LA and Pd/CZL. The α peak can be assigned PdO species nely dispersed on the support and the β peak is attributed to stable PdO particles formed on the interaction between PdO and the support[1,34]. Moreover, the catalytic activity for HC and NO might be related to the reducibility of the α peak[1]. The higher reducibility of nely dispersed PdO species would lead to the higher catalytic activity for HC and NO. In the case of aged catalysts, Pd/CZLA with the lowest reduction temperature of α peak exhibits the best reducibility. Consistent with this result, the aged Pd/CZLA shows the highest catalytic activity.

2.4　XPS studies

Table 2 shows the surface elemental contents calculated from Ce3*d*, Zr3*d*, Al2*p*, La3*d* and O1*s* core level spectra, while Fig.8, Fig.9 and Fig.10 show the Ce3*d*, Pd3*d* and O1*s* XPS spectra for fresh and aged catalysts, respectively.

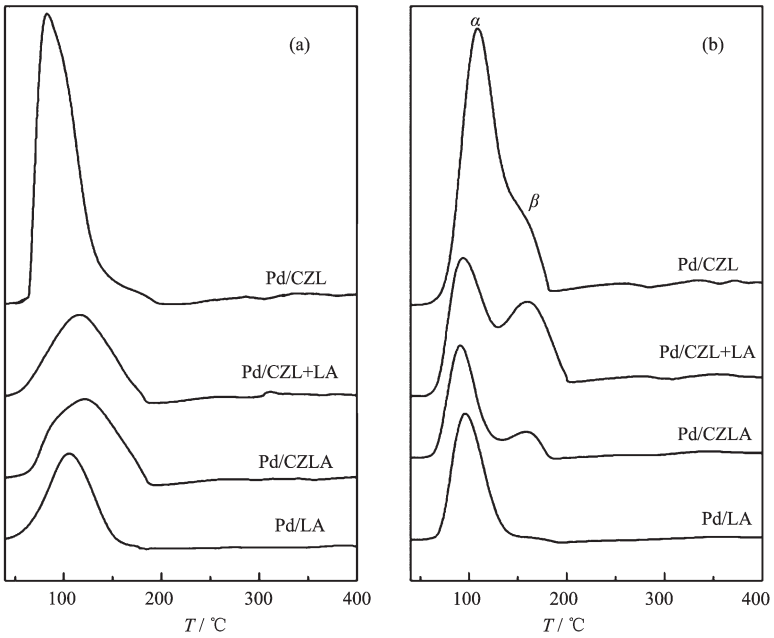

Fig.7 H_2-TPR profiles of the (a) fresh and (b) aged catalysts

Table 2 Data derived from XPS analyses of fresh and aged catalysts

Catalyst		BE / eV	Surface composition / at%					Ce^{3+} in Ce / %
		Pd3$d_{5/2}$	Ce3d	Zr3d	Al2p	La3d	O1s	
Fresh	Pd/LA	336.4	–	–	35.70	0.77	63.53	–
	Pd/CZLA	337.0	0.88	2.66	30.68	0.95	64.83	21.28
	Pd/CZL+LA	336.8	2.50	5.47	26.11	1.37	64.55	19.33
	Pd/CZL	336.5	6.79	13.54	–	2.52	77.15	14.55
Aged	Pd/LA	335.6	–	–	36.07	0.65	63.28	–
	Pd/CZLA	336.4	1.01	2.60	31.87	0.83	63.70	20.37
	Pd/CZL+LA	336.1	1.57	4.81	25.26	2.12	66.24	14.62
	Pd/CZL	335.8	5.14	15.19	–	4.12	75.54	8.47

For fresh ceria-containing catalysts, the surface cerium content increases with the increase of cerium content in supports. After aging treatment, the surface cerium content for the aged catalysts Pd/CZL+LA and Pd/CZL decreases compared with that of fresh catalysts, while it increases for Pd/CZLA. This result indicates that the CZLA exhibits excellent reduction property after aging treatment. Additionally, before and after aging, the surface zirconium contents of CZLA are nearly unchanged.

As shown in Fig.8, the Ce3d spectra are composed of eight peaks no matter in fresh or aged catalysts. The peaks u arise from Ce3$d_{3/2}$, while the others peaks v represent Ce3$d_{5/2}$. The bands labeled as v_1 and u_1 represent the $3d^{10}4f^1$ initial electronic state corresponding to Ce^{3+}, while the peaks labeled as u_3 and v_3 represent the $3d^{10}4f^0$ state of Ce^{4+} ions[35-36]. Table 2 shows the relative concentrations of Ce^{3+} in Ce obtained from the ratio of the sum of peak areas of Ce^{3+} (v_1 and u_1) to the total peak areas of all cerium species. For fresh catalysts, the relative concentrations of Ce^{3+} in Ce increase in the order of Pd/CZLA>Pd/CZL+LA>Pd/CZL. The relative concentration of Ce^{3+} in Ce decrease for aged catalysts, which is mostly related to the sintering of the supports and the reduction of noble metal by the cerium [37], but aged

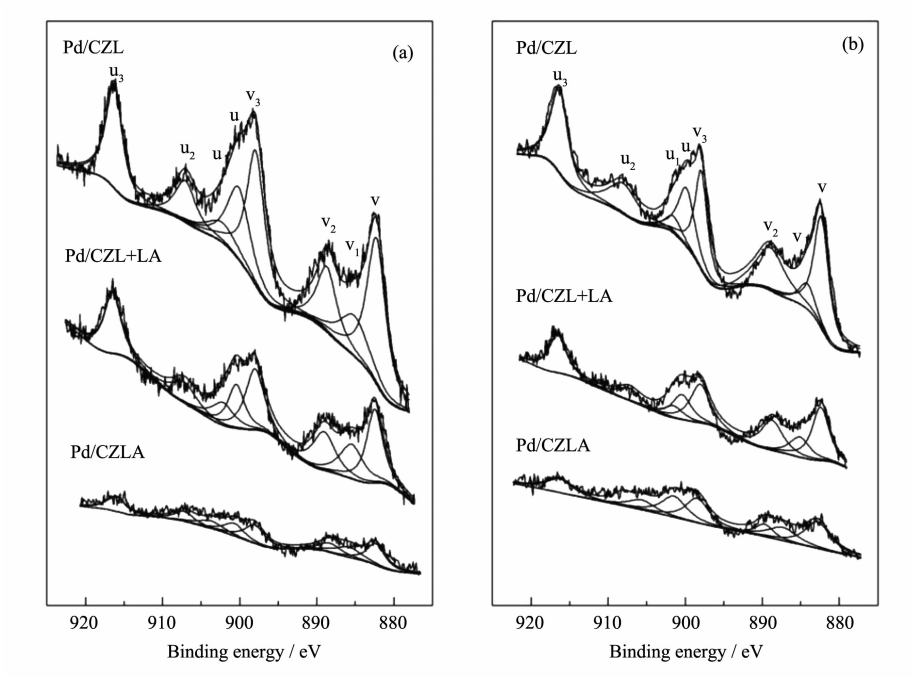

Fig.8　Ce3*d* XPS spectra for the (a) fresh and (b) aged catalysts

Pd/CZLA still shows the biggest value. Generally, the presence of Ce^{3+} is associated with the formation of oxygen vacancies[38]. Furthermore, the oxygen vacancies associated with Ce^{3+} ions adjacent to the noble metal particles are generally consider as the active sites for NO activation[39]. Although the surface Ce concentration is relatively low, the highest relative concentration of Ce^{3+} is obtained for Pd/CZLA, which coincides with the best reduction activity of NO_x.

Fig.9 shows the Pd3*d* XPS spectra for fresh and aged catalysts. Apparently, the pronounced $Zr2p_{1/2}$ and $Zr2p_{3/2}$ signals (345.9 eV and 332.5 eV) partially overlap with the Pd signals, which makes it difficult to quantify the surface palladium concentration. The

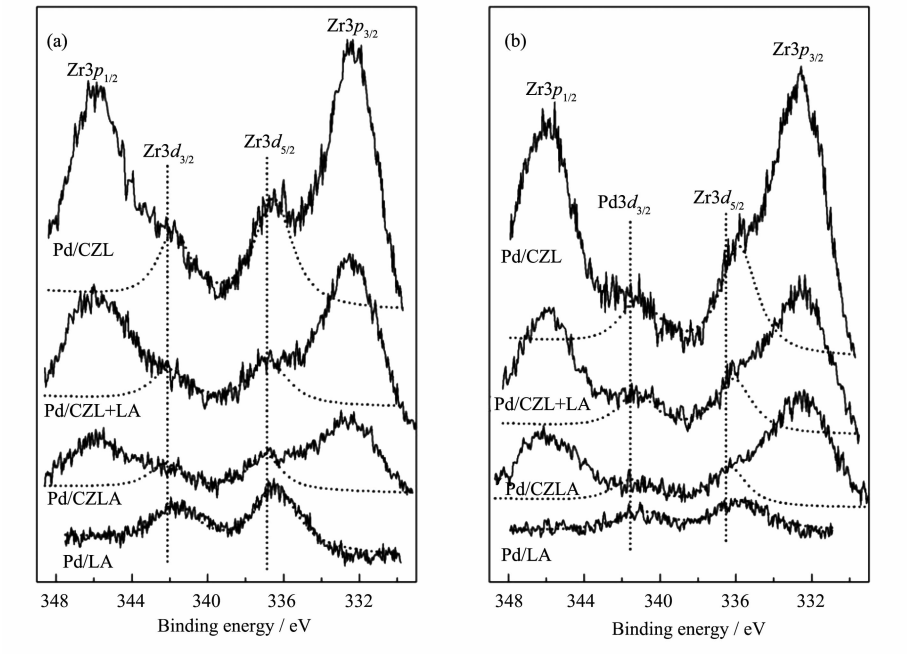

Fig.9　Pd3*d* XPS spectra for the (a) fresh and (b) aged catalysts

values of the binding energies for Pd3$d_{5/2}$ are listed in Table 2. The values are in the order of Pd/CZLA>Pd/CZL+LA>Pd/CZL>Pd/LA, indicating that the chemical state of palladium shifts from oxidic to metallic[40]. This is disadvantageous for catalytic property, because PdO is the active site of TWC[10]. In case of the fresh catalysts Pd/CZLA, the binding energy (BE) value for Pd3$d_{5/2}$ is higher than that of PdO (336.8 eV)[30], implying that Pd^{2+} ions in the present catalysts are much more cationic than PdO. This is helpful to enhance the catalytic activity of TWCs. After aging treatment, palladium signals shift to lower binding energy. For aged Pd/LA, the binding energy (335.6 eV) for Pd3$d_{5/2}$ is almost close to that of reduced Pd^0 signal (335.4 eV)[41], while it is 336.36 eV for Pd/CZLA which still maintains the oxidic state. The transfer of oxygen from the support to the metal can help maintain the Pd in active cationic state[42]. Furthermore, the reduction of Pd oxide can be retarded through a strong metal-support interaction (Pd-O-Ce) effect which takes place easily between highly dispersed PdO particles and CeO_2[43]. Accordingly, the high PdO dispersion of Pd/CZLA (discussed in section 2.5) is easier to form the Pd-O-Ce, which is in favor of keeping the Pd in oxidic state. Owing to this result, the aged Pd/CZLA still keep higher catalytic activity.

The XPS peaks of O1*s* and their peak fittings are displayed in Fig.10. The O1*s* lines of all catalysts can be fitted into three peaks. The first peaks at 529.4~530.0 eV are assigned to the lattice oxygen, denoted as O_I[44]. The second peaks at 530.9~531.3 eV can be attributed to adsorbed oxygen and weakly bonded oxygen species, labeled as O_{II}. And the other peaks at 532.3~532.8 eV are belonged to the surface oxygen by hydroxyl species and adsorbed water species, labeled as O_{III}[36]. Usually, adsorbed oxygen (O_{II}) is considered to be more reactive than others due to the former has higher mobility[45]. It is often known that more active oxygen is beneficial for catalytic activity of TWCs. The O_{II} ratios, calculated by $O_{II}/(O_I+O_{II}+O_{III})$ are shown in Fig.10. For fresh catalysts, Pd/CZLA is provided with the most active oxygen among all catalysts, while the Pd/CZL exhibits the lowest amount of active oxygen. Although catalyst Pd/LA is provided with relatively more active oxygen, the absence of oxygen storage property for LA leads to the poor catalytic activity of Pd/LA. As for aged catalysts, the amount of active oxygen decrease for all catalysts due to sintering, but Pd/CZLA still remains more active oxygen than others. This result is in line with catalytic activity discussed above and provides a reason for the excellent catalytic activity of Pd/CZLA.

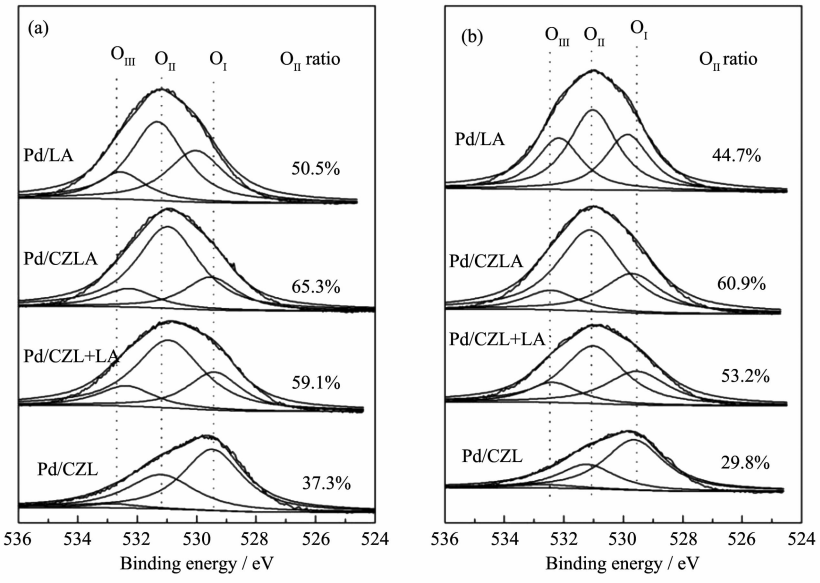

Fig.10 O1*s* XPS spectra for the (a) fresh and (b) aged catalysts

2.5 CO chemisorption

The dispersion of active metal component is an important parameter of supported metal catalysts and the dispersions of active PdO_x in fresh and aged catalysts are determined by CO chemisorption. The average particle size according to D is obtained by d (nm) $\approx 1.1/D$[46], where D is the dispersion of Pd. The D is calculated using the formula $V_0 \cdot M_{Pd} \cdot 10^{-3}/(22.4w \cdot p)$, where V_0 is the consumption of CO (mL), w is the mass of catalyst, p is the mass fraction of Pd, and M_{Pd} is molecular weight of Pd (106.4 g·mol^{-1})[47]. The results are listed in Table 3. It is obvious that Pd/CZLA exhibits higher Pd dispersion and smaller particle size than other three catalysts no matter fresh and aged catalyst. As reported in previous study[48], Pd dispersion is not only related to the specific surface area, but also associated with interaction between the catalyst and the support. Therefore, the higher Pd dispersion of Pd/CZLA is ascribed to the higher surface area of CZLA and the formation of a strong metal-support interaction (Pd-O-Ce). The higher Pd dispersion and smaller particle size imply to form fine and/or ultrafine particles producing higher active surface, so that the catalytic activity will be enhanced[49]. The measured extents of Pd dispersion are in good agreement with the catalytic activity.

Table 3 Results of CO chemisorption for fresh and aged catalysts

Catalyst	Fresh		Aged	
	Pd dispersion / %	Pd particle size / nm	Pd dispersion / %	Pd particle size / nm
Pd/LA	16.3	6.7	2.8	39.3
Pd/CZLA	23.5	4.7	6.1	18.0
Pd/CZL+LA	17.4	6.3	4.4	25.0
Pd/CZL	16.3	6.7	3.2	34.4

3 Conclusions

In summary, different supports lead to different textural properties. The absence of oxygen storage capacity for LA makes it the worst support of the Pd-only three-way catalyst. Besides, among ceria-containing supports, CZLA exhibits the highest surface area, biggest pore volume as well as widest pore size distribution, moreover, it shows excellent thermal stability at high temperature. This result indicates that the introduction of Al into the CZ solid solution leads to the improvement of textural properties and thermostability.

Support CZLA exhibits superior reducibility before and after aging due to its excellent thermal stability. Additionally, catalyst Pd/CZLA shows high reducibility of PdO species finely dispersed on the support, which is beneficial to the catalytic activity.

For Pd/CZLA, the formation of the strong metal-support interaction (Pd-O-Ce) in the Pd-CeO_2 interface maintains the Pd in a more active state.

Based on the above advantages, CZLA as support material of the Pd-only three-way catalyst amplifies the amplitude of air/fuel operation window and improves catalytic activity.

References:

[1] Wang Q Y, Li G F, Zhao B, et al. *Appl. Catal. B*: *Environ.*, **2010**,**101**(1/2):150-159

[2] Matsumoto S I. *Catal. Today*, **2004**,**90**(3/4):183-190

[3] Shelef M, McCabe R W. *Catal. Today*, **2000**,**62**(1):35-50

[4] Kašpar J, Fornasiero P. *J. Solid State Chem.*, **2003**,**171**(1/2): 19-29

[5] Farrauto R J, Heck R M. *Catal. Today*, **1999**,**51**(3/4):351-360

[6] Tomaš ić V, Jović F. *Appl. Catal. A*: *Gen.*, **2006**,**311**:112-121

[7] Gandhi H S, Graham G W, McCabe R W. *J. Catal.*, **2003**, **216**(1/2):433-442

[8] Lan L, Chen S H, Zhao M, et al. *J. Mol. Catal. A*:*Chem.* **2014**,**394**:10-21

[9] Talo A, Lahtinen J, Hautojärvi P. *Appl. Catal. B*:*Environ.*, **1995**,**5**(3):221-231

[10]CAI Li(蔡黎), CHEN Shan-Hu(陈山虎), ZHAO Ming(赵明), et al. *Chinese J. Inorg. Chem.*(无机化学学报), **2009**,**25**(3): 474-479

[11]Iwamoto M, Zengyo T, Hernandez A M, et al. *Appl.Catal. B*:

Environ., **1998**,**17**(3):259-266

[12]Kolli T, Lassi U, Rahkamaa-Tolonen K, et al. *Appl. Catal. A*: *Gen.*, **2006**,**298**:65-72

[13]HE Sheng-Nan(何胜楠), CUI Ya-Juan(崔亚娟), YAO Yan-Ling(姚艳玲), et al. *Acta Phys.-Chim. Sin.*(物理化学学报), **2011**,**27**(5):1157-1162

[14]Wilcox L, Burnside G, Kiranga B, et al. *Chem. Mater.*, **2003**, 15(1):51-56

[15]Kašpar J, Fornasiero P, Hickey N. *Catal. Today*, **2003**,**77**(4): 419-449

[16]Kašpar J, Fornasiero P, Graziani M. *Catal. Today*, **1999**,**50** (2):285-298

[17]Morikawa A, Suzuki T, Kanazawa T, et al. *Appl. Catal. B*: *Environ.*, **2008**,**78**(3/4)210-221

[18]CUI Ya-Juan(崔亚娟), HE Sheng-Nan(何胜楠), FANG Rui-Mei(方瑞梅), et al. *Chinese. J. Catal.*(催化学报), **2013**,**33** (6):1020-1026

[19]WANG Xing-Yi(王幸宜), LU Guan-Zhong(卢冠忠), JIN Liu-Wei(金柳伟). *J. Chinese Rare Earth Soc.*(中国稀土学报), **1995**,**13**(2):128-131

[20]Papavasiliou A, Tsetsekou A, Matsouka V, et al. *Appl. Catal. B*: *Environ.*, **2009**,**90**(1/2):162-174

[21]Li C L, Gu X, Wang Y Q, et al. *J. Rare Earth*, **2009**,**27**(2): 211-215

[22]López Granados M, Gurbani A, Mariscal R, et al. *J. Catal.*, **2008**,**256**(2):172-182

[23]Leofanti G, Padovan M, Tozzola G, et al. *Catal. Today*, **1998**, **41**(1/2/3):207-219

[24]Wang Q Y, Zhao B, Li G F, et al. *Environ. Sci. Technol*, **2010**,**44**(10):3870-3875

[25]Jen H W, Graham G W, Chun W, et al. *Catal. Today*, **1999**, **50**(2):309-328

[26]TANG Shi-Yun(唐石云), JIAO Yi(焦毅), LI Xiao-Shuang(李小双), et al. *Chinese J. Inorg. Chem.*(无机化学学报), **2012**,**28**(5):965-970

[27]Rumruangwong M, Wongkasemjit S. *Appl. Organomet. Chem.*, **2006**,**20**(10):615-625

[28]Mejía-Centeno I, Castillo S, Fuentes G A. *Appl. Catal. B:Environ.*, ***2012***,119-120:234-240

[29]Guo Y, Lu G Z, Zhang Z G, et al. *Catal. Today*, **2007**,**126**(3/4):296-302

[30]Sun K P, Lu W W, Wang M, et al. *Appl. Catal. A:Gen.*, **2004**,**268**(1/2):107-113

[31]Barrera A, Viniegra M, Fuentes S, et al. *Appl. Catal. B*: *Environ.*, **2005**,**56**(4),279-288

[32]Luo M F, Zheng X M. *Appl. Catal. A:Gen.*, **1999**,**189**(1):15-21

[33]Costa C N, Christou S Y, Georgiou G, et al. *J. Catal.*, **2003**, 219(2):259-272

[34]Lambrou P S, Efatathiou A M. *J. Catal.*, **2006**,**240** (2): 182-193

[35]Li G F, Wang Q Y, Zhao B, et al. *Appl. Catal. B:Environ.*, **2011**,**105**(1/2):151-162

[36]Nelson A E, Schulz K H. *Appl. Surf. Sci.*, **2003**,**210**(3/4): 206-221

[37]Zhao B, Li G F, Ge C H, et al. *Appl. Catal. B:Environ.*, **2010**,**96**(3/4):338-349

[38]Bozo C, Guilhaume N, Herrmann J M. *J. Catal.*, **2001**,**203** (2):393-406

[39]Polona V, Fornasiero P, Kašpar J, et al. *J. Catal.*, **1997**, **171**(1):160-168

[40]Winkler A, Dimopoulos P, Hauert R, et al. *Appl. Catal. B*: *Environ.*, **2008**,**84**(1/2):162-169

[41]Weng X L, Zhang J Y, Wu Z B, et al. *Appl. Catal. B*: *Environ.*, **2011**,**103**(3/4):453-461

[42]Liu Y Y, Hayakawa T, Ishii T, et al. *Appl. Catal. A:Gen.*, **2001**,**210**(1/2):301-314

[43]Hu Z, Wan C Z, Lui Y K, et al. *Catal. Today*, **1996**,**30**(1/2/3):83-89

[44]He H, Dai H X, Au C T. *Catal. Today*, **2004**,**90**(3/4):245-254

[45]Wang X Y, Kang Q, Li D. *Appl. Catal. B:Environ.*, **2009**, **86**(3/4):166-175

[46]Bourane A, Derrouiche S, Bianchi D. *J. Catal.*, **2004**,**228** (2):288-297

[47]YANG Chun-Yan(杨春雁), YANG Wei-Ya(杨卫亚), LING Feng-Xiang(凌凤香), et al. *Chem. Ind. Eng. Prog.*(化工进展), **2010**,**29**(8):1468-1473

[48]Sekizawa K, Widjaja H, Maeda S, et al. *Appl. Catal. A*: *Gen.*, **2000**,**200**(1/2):211-217

[49]SHANG Hong-Yan(尚鸿燕), WAGN Yun(王云), GONG Mao-Chu(龚茂初), et al. *J. Energ. Chem.*(能源化学:英文版), **2012**,**21**(4):393-399